Dowel type joints – Influence of moisture changes and dowel surface smoothness

Erik Serrano and Johan Sjödin, Växjö University, Sweden

Background and introduction

With the increased use of glulam in large-span timber structures, the interest from engineers and the research community has also been very pronounced in recent years. A numerous amount of research projects, conferences, articles and – not to forget – a seemingly never-ending number of innovative joint designs have been realized. Often, focus has been on the load bearing capacity of joints, the design methods to be used, and how to handle the complex behaviour in the code.

One area, were much less effort has been put, is the behaviour of large timber joints when exposed to moisture variations.

Within an ongoing PhD-programme at Växjö University, Sweden, this subject, and others are being addressed. Thus, research has been and is being performed within areas relating to:

- the influence of moisture changes;
- the influence of moisture gradients within the timber;
- methods to improve joint ductility;
- the influence of dowel-to-timber friction;
- experimental and numerical methods

In Sweden glulam is normally delivered at an average moisture content of 12-14 %. Even if the glulam is being protected from direct rain, the outdoor climate can give some moistening during construction. In winter, the indoor air can be as dry as 20% relative humidity. In combination with the large cross-sectional dimensions in long-span construction and the orthotropic behaviour of the timber, there seems to be an obvious risk of inducing large stresses due to moisture variations.

In the current codes, national and European, a number of service classes are defined. Out of these service classes, one is defined with the same climate as the standard climate used in testing (20/65). Other service classes relate to more moist conditions for which the strength is *reduced*.

With the above, two questions arise:

1. Is there a significant effect of drying from “standard” climates on the load bearing capacity of timber joints?
2. How do the dowel surface smoothness affect the behaviour of the joint?
3. Do the current codes (national or international) take this into account?

The current paper tries to give an overview of some of the ongoing activities and recently performed research addressing items 1 and 2 above, giving also preliminary answers to these questions. The third question is still very much open for discussion.

Overview of test programmes

Four experimental studies within the ongoing PhD-programme are reported here. The first relates to tests on large dowel type joints, where different joint lay-outs and climatic cycles were used to investigate the effect of restrained shrinkage. Further details can be found in (Sjödin and Johansson, 2007).

The second study relates to further tests on the influence of moisture variations. In order to isolate the effect of changing the moisture in the timber from the restrained shrinkage-effect, this study was performed on single-row joints. This study is under publication (has been accepted following minor revisions), and is expected to be published during 2008.

The third study relates to the use of contact-free deformation technique as a tool in understanding the complex behaviour in timber joints. This work has been published, and further details can be found in (Sjödin, Serrano and Enquist, 2006).

The fourth study, finally, relates to an ongoing study on the influence of the friction between dowels and timber in the joint.

The influence of moisture variations on load-bearing capacity

Specimens

Three different joint types have been used in studying the influence of moisture variations on the load-bearing capacity of dowel-type joints. The joint types are shown below in Figure 1.
The difference between the two joint types 1 and 2 lies in the spacing of the dowel rows perpendicular to the grain, which is set to 3d (36 mm) for type 1 and 5d (60 mm) for type 2. The other distances, were set to the minimum values given in EC5. The thickness of glulam on either side of the steel plate in all specimens was 30 mm. The dowels were 12 mm in diameter, with a tolerance of ± 0.2 mm. The holes in the steel plates were cut out by laser, their being 12.2 mm in diameter, with a tolerance of ± 0.1 mm. The steel plates were used as templates when drilling the holes in the timber. All the specimens were stored in a standard climate of 20ºC and 65% relative humidity (RH) until an equilibrium MC of 12% (±0.6%) was reached, prior to further preparation.

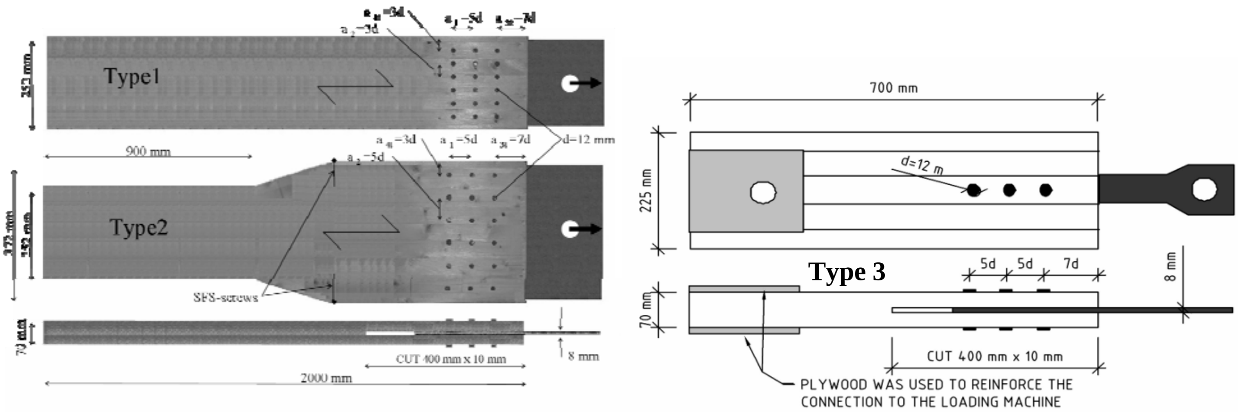

Figure 1. Two types of multiple-row joints (left) and one type of single-row joints have been used.

Climatic conditions and joint preparation sequences

A total of 30 specimens of type 1 and 2 were employed (15 specimens for each of the two types of joints). These specimens were divided into three categories, A, B and C. For the type 3 joints, a total of 25 specimens were used, divided into categories A (5) and B1-B5 (4 each). The three categories A, B and C, differed in the climate conditions to which the specimens were subjected and when the steel plate and the dowels were fitted into the specimens. Specifically, the characteristics of the three categories were as follows:

- For category A the steel plate and the steel dowels were fitted into the specimens when a 12% equilibrium moisture content had been reached in a 20ºC, 65% RH climate, after which the specimens were loaded to failure.
- For category B the climate conditions were somewhat drier. After an equilibrium moisture content of 12 % had been reached, the specimens were stored at 20ºC, 30% RH for type 1 and 2 and 20ºC, 20% RH for type 3 respectively. The specimens were kept in the dry climate for approximately 110 days for type 1 and 2. The type 3 joints were kept in the somewhat drier climate for 3, 7, 14, or 60 days. After drying, the steel plate and the steel dowels were fitted in to them. The specimens were then loaded to failure.
- For category C the steel plate and the steel dowels were fitted into the specimens when an equilibrium moisture content of 12% had been reached. The climate was then changed from the initial climate of 20ºC, 65% RH to one of 20ºC, 30% RH. This climate maintained was kept for approximately 110 days before the specimens were loaded to failure.

The climate conditions for category A were chosen in such a way of to simulate standard procedures used in testing joints and to employ the results obtained for this category as a reference. The climate change for categories B and C was chosen to simulate a reasonably realistic change in climate. Nordic glulam beams are normally delivered from the manufactures with an MC of about 12 %, corresponding to the standard climate of 20ºC, 65% RH used in the present study. During storage in the climate chambers the cross-section perpendicular to the grain was measured at three different locations in order to study the shrinkage deformations.

Results – Type 1 and 2

The results for the type 1 and 2 joints is summarized in Table 1 and Figure 2 below, details are given in Appendix, indicating also the failure modes obtained.

Table 1. Mean and relative load-bearing capacity, type 1 and 2.

	Category	Row spacing	Mean capacity [kN]	Relative capacity
Type1	A	3d	313	1
	B	3d	290	0,93
	C	3d	248	0,79
Type2	A	5d	375	1
	B	5d	315	0,84
	C	5d	277	0,74

The basic difference between categories A and B in terms of the conditions involved concerned the moisture content at the time of the fitting of the steel plates and dowels, the moisture content being higher for category A. Thus, the mean load-bearing capacity was greater for the category A than for the category B specimens, i.e. for those specimens that had a higher moisture content.

A possible explanation to the behaviour found for category B is that internal stresses have developed during drying from about 12 % to 8 % MC. Another explanation might be in terms of internal stresses being induced in the area of the connection depending on the orientation of the annual rings.

Differences between categories B and C were the earlier insertion of the dowels and the plate in the specimens belonging to category C. Greater internal stresses were due to that expected for this category due to restrained shrinkage deformations by the dowels and the plate during storage in the climate chamber. The results show that the specimens belonging to category C is affected by this, i.e. the mean load-bearing capacity is lower for specimens belonging to category C then of category B. The specimens belonging to type 2 show a higher decrease in the mean load-bearing capacity than type 1 specimens when comparing the results between category A and C. One should note that it is sometimes remarked in the literature that joints with large row spacing tend to be underestimated in design codes, see Quenneville and Mohammad (2000) for example.

According to Eurocode 5, all the above joints should have the same capacity, the actual influence for the different joints is shown below.

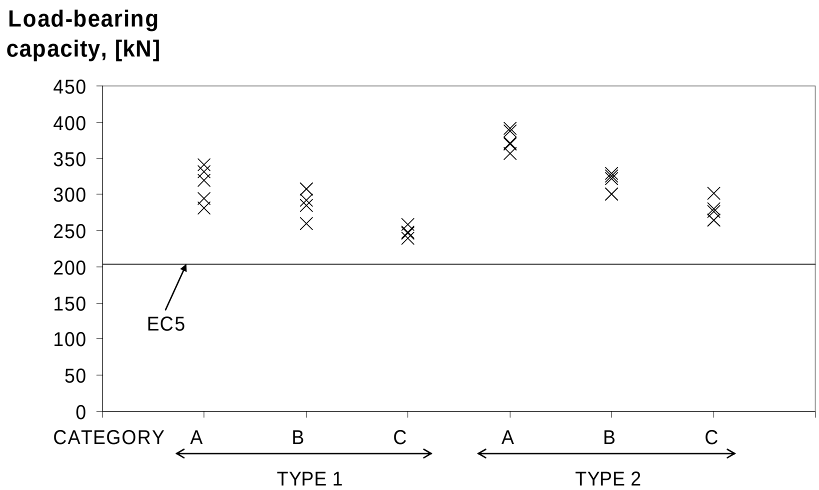

Figure 2. Load bearing capacity of tested joints type 1 and 2.

Results – Type 3

A typical failure mode, characteristic for all specimens, was difficult to define. Usually, a combination of splitting failure and plug shear failure was seen. With one or two exceptions for all the specimens belonging to category B1-B5, no distinct ductile behaviour could be observed. Instead, failure occurred rather suddenly at the ultimate load, showing small plastic displacements. For the specimens belonging to the reference category A1, however, a more ductile behaviour is indicated, i.e. the plastic displacement being generally larger at failure.

The results are summarized below in terms of load-bearing capacities, details are found in Appendix. The results show the effect of the climate change to be in the range of 5-15 % lower load bearing capacity. Note that, due to the joint manufacturing and testing sequence used, the present joints are not subject to constraint stresses (due to hindered drying deformations perpendicular to the grain by the steel dowels and the steel plate). In cases of larger joints with multiple rows of dowels, such hindered shrinkage deformations would affect the load-bearing capacity even more; see above section with joints type 1 and 2. Thus. one possible explanation to the behaviour is that stresses induced by moisture gradients have developed in the joint area for the specimen exposed to drying. Thus, it is also likely that small cracks have been initiated in the joint area.

Table 2. Load bearing capacities, type 3 joints.

Type	Mean (kN)	Relative capacity
A1	59	1.00
B1	56	0.94
B2	51	0.86
B3	54	0.92
B4	50	0.85
B5	52	0.88

Contact free deformation technique for dowel type joints testing

Despite the fact that theoretical methods can provide detailed results, it is still rather unusual in experimental studies of joints to gather data other than that of a joints global load-displacement response. Modern contact-free measurement techniques are possible to employ in order to fill this gap.

In order to gain a better understanding of the overall performance of timber joints, a large area around the joint needs to be studied. This is possible today thanks to advanced contact-free measurement systems often commercialized and frequently used as established techniques in areas other than timber engineering. Advantages of these new systems include the possibility of determining deformations and strains within large areas, and of maintaining a high level of accuracy and spatial resolution in a large number of separate instances during loading. Also, such systems can simultaneously record data such as load and displacement readings from the loading machine. In systems of this sort, which in addition are user–friendly, strong efforts have been directed at making it easy to evaluate the measurement data.

Specimens and set-up

The measurement system ARAMIS^{TM} manufactured by the company GOM was employed. The system is based on evaluating a random or regular pattern, which is applied to the surface and deforms along with the material. The placing of two CCD cameras (1280 by 1024 resolution) in front of the specimen at different angles enables stereoscopic pictures of the patterned surface, to be taken at different occasions during loading, see Figure 3.

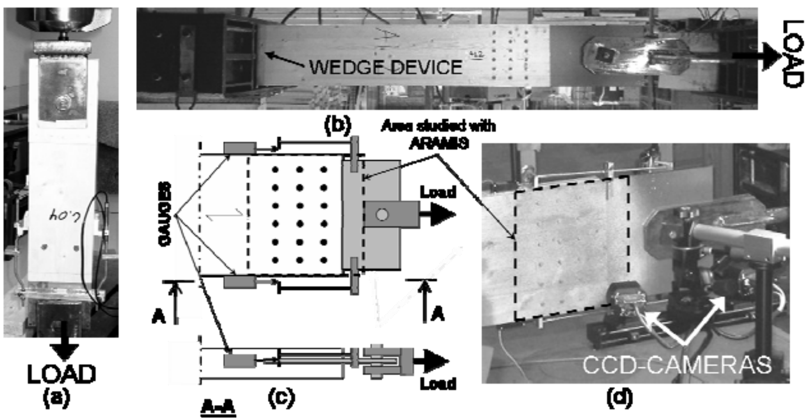

Figure 3. **(a) Load-setup for type 1 joints, (b) load-setup for type 2 joints, (c) application of inductive gauges (similar in the case of both types) and (d) type 2 joint, in to which random patterns are applied, and the CCD-cameras used.**

The first digital-image processing step defines macro-image facets in the image pair in the original, unloaded state. For each stage of loading, the 3D coordinates of these facets on the specimen's surface are calculated accurately using image correlation and photogrammetric principles. On the bases of these 3D coordinates, the 3D displacements and in-plane strains as well as the shape of the specimen can be calculated with a high degree of spatial resolution.

The test arrangements for all the joints were similar. The CCD cameras were calibrated to a measurement volume that included the joint area and part of the steel plate; see the area inside the dashed lines in Figure 3. A random pattern was achieved in two steps. First a matt light-coloured paint was sprayed on the area around the dowels. This was done in order to obtain better contrast of the grey scale defining the facets and also to reduce the shininess of the timber. After this, small black dots were applied by spraying black paint at the surface from a distance.

The cameras were triggered every five seconds, also logging signal readings of displacement and force from the loading machine. The test images were then processed by the software, which is included the ARAMIS-system. For each pair of images, 3D coordinates for a large number of facets could be determined and be converted to relative displacements and strains. The calibration volume selected results in a spatial resolution of 3-4 mm for the two joint types tested, see Figure 4-5. According to the manufacturer, the strain accuracy is approximately 0.02%.

Results

The results showed differences in terms of joint ductility and failure modes (and of course load bearing capacities). However, since the purpose here is mainly to show the potential of using the contact-free deformation technique, results are presented in terms of strain distributions only. Details are available in the original article (Sjödin, Serrano and Enquist, 2006).

The strain distributions in the joint area for the two types of joints are presented below in Figure 4-5. The results obtained by the ARAMIS-system were taken in the elastic region just before the joints indicated plastic behaviour in the global load-displacement response, involving a total load of approximately 28kN and 270kN for the two joint types respectively. For comparison, these results are shown together with those from numerical analyses at the same load level. The results were not compared in the plastic range since the numerical analyses dealt only with elastic behaviour.

It should be emphasized that only the surface on one side of the joints was studied with the ARAMIS-system. Due to that it is possible that, for example, cracks may have occurred on the opposite side of the joints.

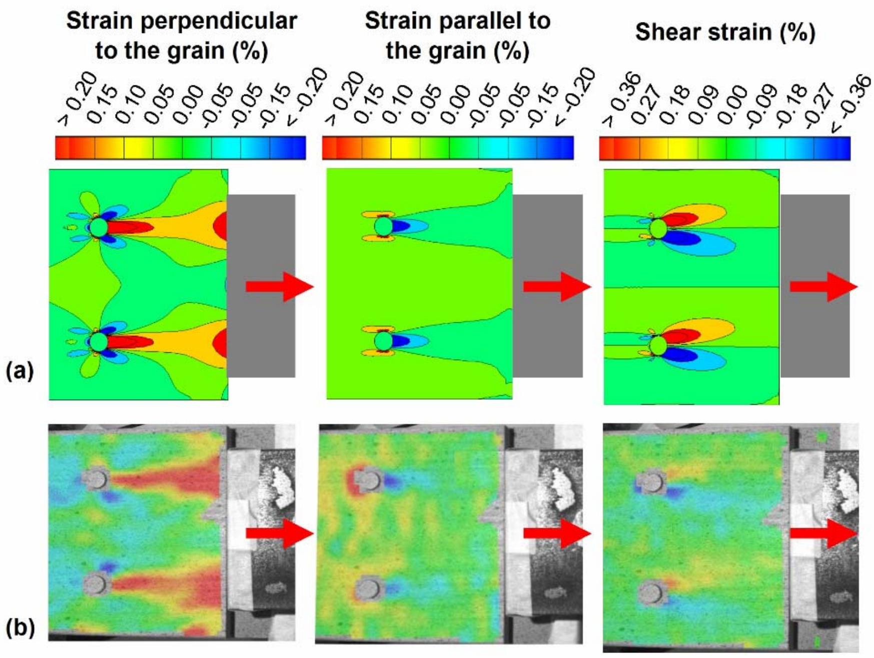

Figure 4 Strain distributions in the joint area at 28kN: (a) numerical results, (b) results from the ARAMIS-system.

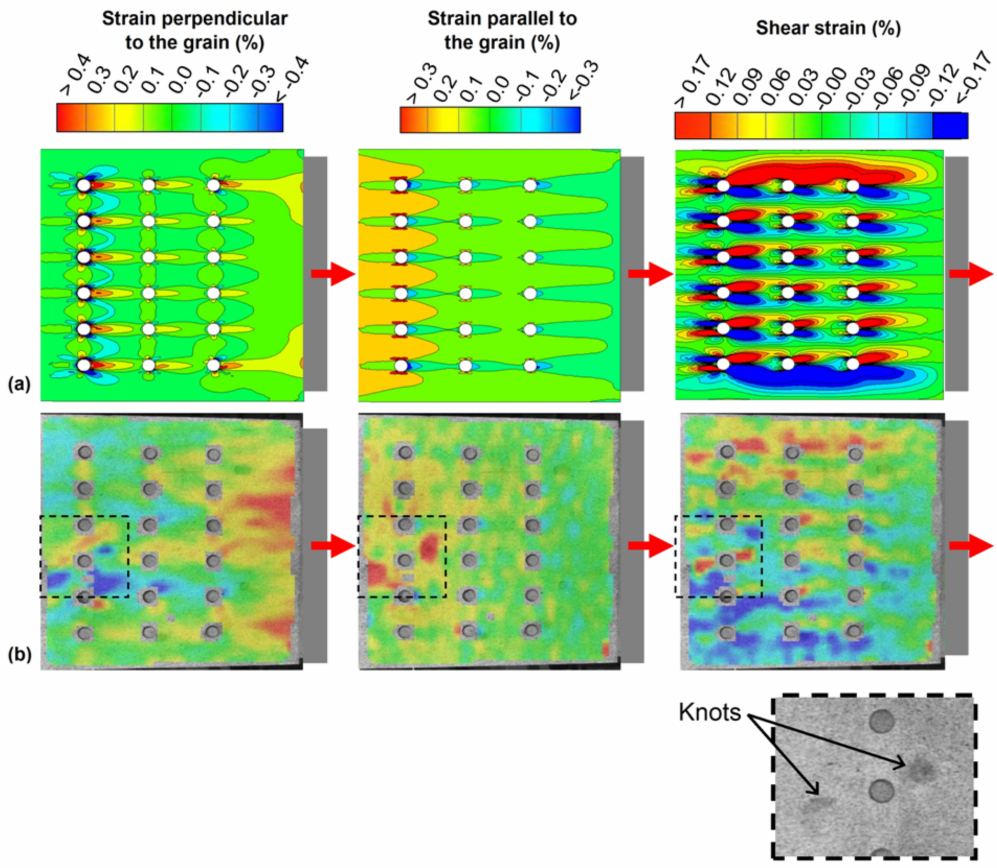

Figure 5. Strain distributions in the joint area at 270 kN: (a) numerical results, (b) results from the ARAMIS-system and presence of knots in the areas inside the dashed lines.

The effect of friction between the dowel and timber in single dowel joints

The design rules contained in the European timber code EC5 (Eurocode 5, 2004) for single bolted joints loaded parallel to the grain are based on the Johansen yielding theory (Johansen 1949), which assumes a rigid plastic behaviour of the timber and the dowels. Restrictions related to end and edge distances and timber thickness are also included in EC5 in order to help avoid brittle failure modes. One important parameter to determine in order to be able to adopt design equations is the embedment strength of timber. Blass (2003) listed several parameters that affects the embedment strength of timber, e.g., the timber density, the dowel and the hole diameter; angle between the load and the grain direction and the moisture content. Another parameter, which is considered in the present paper, is the effect of friction between the dowel and the surrounding timber. Extensive experimental and some theoretical works have been made in this area (Rodd 1973; Siem 1999). Results have showed that increasing surface roughness of the dowels increases the embedment strength; reduces the brittle tendencies of the joints; changes the location of the initial crack/cracks and affects the type of finally brittle failure mode.

As shown above, a complicated strain- and thereby stress distribution in the area close to the dowels exists. This behaviour is rather difficult to study by both experimental and theoretical approaches, implying that the behaviour of dowel type joints and further the effect of friction between to dowel and the surrounding timber are not fully understood yet. Contact-free measurements might therefore be one experimental method in order to increase the knowledge of dowel-type joints.

In this partly experimental and partly numerically study, the same contact free measurement system as described briefly above was used for studying the joint area in single dowel joints loaded in tension parallel to the grain.

The joints studied are divided into two groups of joints where the surface of the dowel is different. For group 1, the dowels have a smooth surface and for group 2, the dowels have a rough surface. The primary aim was to study the effect of friction between the dowel and the surrounding timber closely. The aim was further to estimate the coefficient of friction for respectively group by comparing experimental and numerical results.

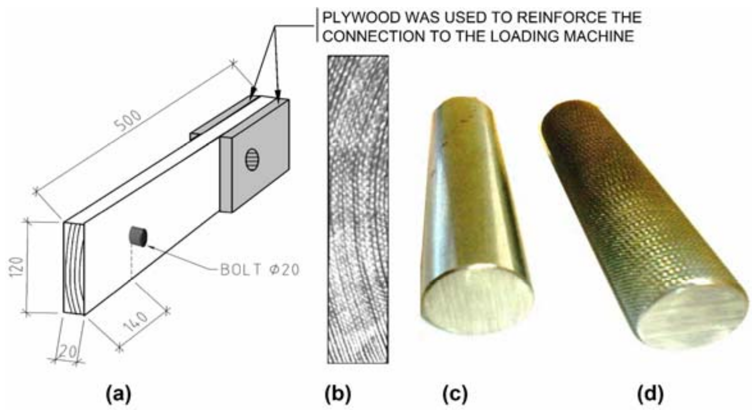

Figure 6. a) Set-up, b) the orientation of the annual rings for the timber, c) a smooth dowel, d) a dowel with a rough surface.

Results

The load-displacement curves presented in Figure 7 for all joints tested are based on the mean value of the displacement readings of the two inductive gauges applied to each joint.

The results concerning the joints with smooth surface dowels indicate a ductile behaviour. This was not caused by plastic hinges developing in the dowel, but by the embedment failure of the wood in combination with an initial crack located in front of the dowel, Figure 8. This led to a marked local deformation in the timber in the area close to the dowel. The presence of an initial crack close to the dowel is an observation that is supported by previous research (see e.g. Schmid et al 2002; Daudeville et al. 1999). Interesting here was that this crack was initiated at the time when the elastic displacements turned to plastic. The final failure mode was the splitting failure mode, Figure 8. This caused the load to drop almost completely. Note that in some joints the initial crack in front of the dowels seemed to be propagating until to the final failure, whereas in some cases the final failure seemed to be initiated from the end grain

The results for the joints with rough surface dowels were very different when compared to the smooth dowels. Most important differences were that the load-bearing capacities were much higher and the results were much less scattered for the rough dowels, see Figure 8. Furthermore, no initial crack was seen, but only embedment failure of the wood was noticed, see, Figure 8. The final failure mode was the plug-shear failure mode.

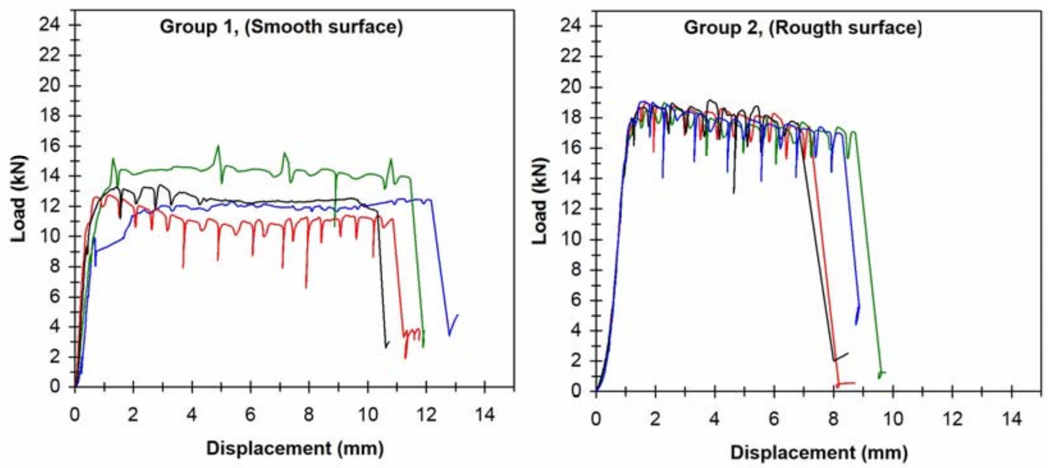

Figure 7. Load-displacement response from tests with smooth dowels (left) and dowels with a rough surface (right).

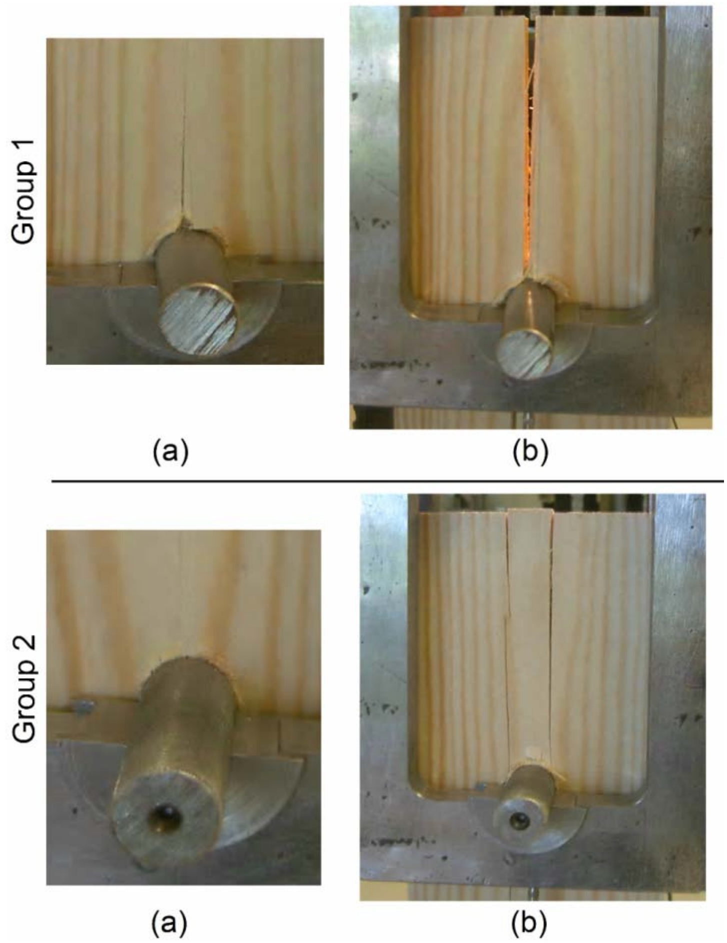

Figure 8 **Failure modes obtained with smooth dowels (group 1) and rough dowels (group 2). A and b denote the instances of initial and final failure respectively.**

The use of the contact free deformation measurement system and finite element analyses, made it possible to estimate the value of the coefficient of friction, μ, between dowels and timber. The resulting strain distributions are shown below. For the smooth dowels, setting the value of μ to 0.1, was found to give a good fit. For the rough dowels, a value of μ=0.4 was found appropriate. Obviously the linear elastic finite element analyses do not take into account a number of complex effects, including the plastic behaviour in the contact zone between dowel and timber. Thus, fitting the strain fields by the single parameter μ, could be questioned. Nevertheless, the current study shows, in addition to effect of the friction on the load bearing capacity, the potential of the contact free measurement technique to perform detailed studies of the constitutive behaviour of the timber.

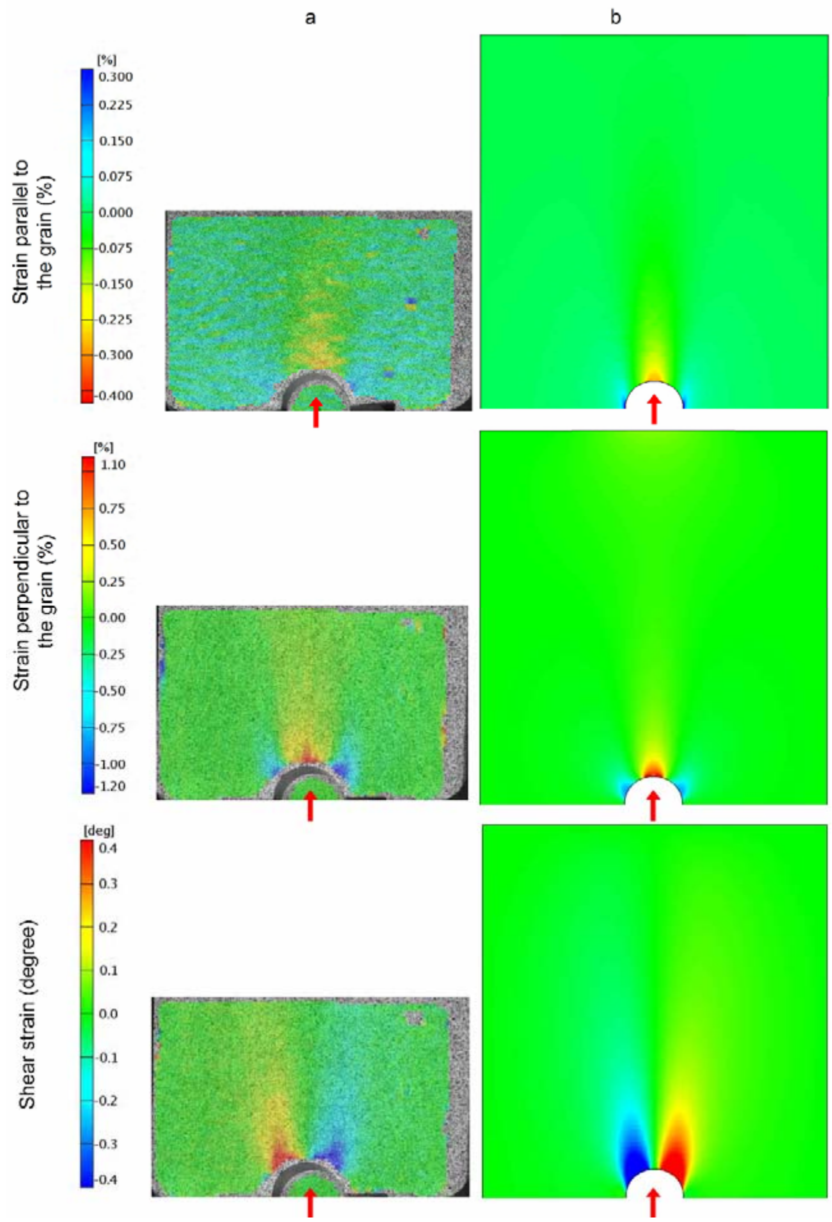

Figure 9. **Strain distribution in the joint area at 11 kN (smooth dowels): a) results from the ARAMIS-system, b) numerical results where μ is set to 0.1.**

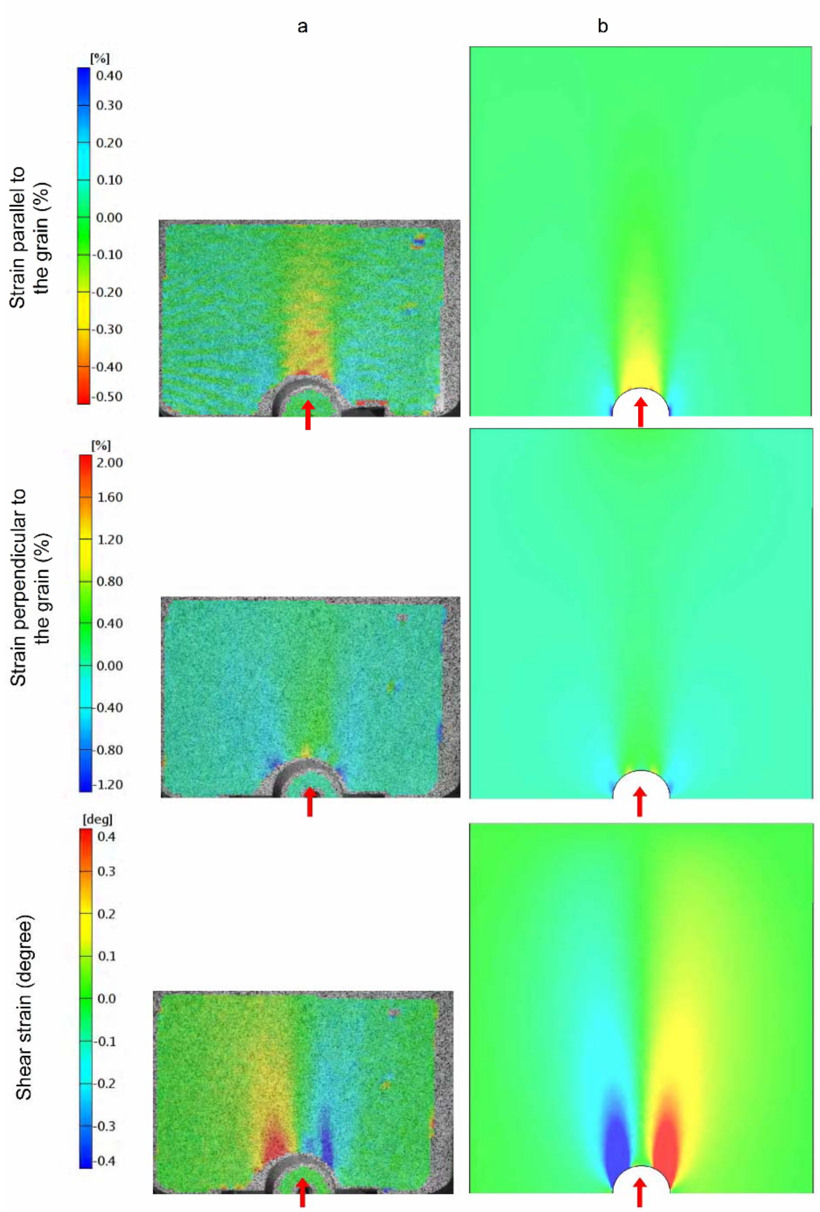

Figure 10. Strain distribution in the joint area at 17 kN (rough dowels): a) results from the ARAMIS-system, b) numerical results where m is set to 0.4.

References

Blass, H. J. (2003) Joints with dowel-type fasteners. In Timber Engineering. Thelandersson and Larsen, H.J., Eds, Wiley & Sons, ISBN 0-470-84469-8.

Daudeville, L., Davenne, L., and Yasumura, M. (1999) Prediction of the load carrying capacity of bolted timber joints. Wood Science and Technology. 33(1): 15-29

Eurocode 5. (2004) Eurocode 5 - Design of timber structures. EN 1995-1-1:2004(E).

Johansen, K.W. (1949) Theory of timber connections. International Association of Bridge and Strucural Engineering 9:, 249-262

Quenneville, J. H. P., and Mohammad, M. (2000) On the failure modes and strength of steel-to-timber bolted connections loaded parallel-to-grain. Can. J. Eng., 27, 761-773.

Rodd, P. D. (1973) The analysis of timber joints made with circular dowel connectors. Ph.D. thesis, University of Sussex, England.

Schmid, M., Blass, H. J., and Frasson, R. P. M. (2002) Effect of distances, spacing and number of dowels in a row on the load carrying capacity of connections with dowels failing by splitting. Proceedings of the CIB W18 Meeting, paper CIB-W18/31-9-1, Kyoto, Japan.

Siem, J. (1999) Capacity and ductility of dowel connections in timber structures (In Norwegian). Ph.D. thesis, Norwegian University of Science and Technology, 1999:46, ISSN 0802-5271.

Sjödin, J., and Johansson, C-J. (2007) Influence of initial moisture induced stresses in multiple steel-to-timber dowel joints. Holz als Roh- und Werkstoff 65: 71–77. (DOI 10.1007/s00107-006-0136-6)

Sjödin. J., Serrano, E. and Enquist, B. Contact-free measurements and numerical analyses of the strain distribution in the joint area of steel-to-timber dowel joints. Holz als Roh- und Werkstoff 64: 497–506. (DOI 10.1007/s00107-006-0112-1)

Appendix 1 – Test conditions and experimental results.

Type 1 and 2

Category	Type	Specimen	Humidity conditions Step1*	Humidity conditions Step2**	MC just after the specimens were loaded to failure	Time at which plate and dowels were fitted to the specimens	Visible defects produced by moisture reduction	Load-bearing capacity [kN]	Mean capacity [kN]	COV [%]	Failure mode
A	1	1			11,8%		-	294			BS/RS
		2			11,4%		-	320			RS
		3			12,2%		-	331	313	8,0	BS/RS
		4			11,7%		-	281			BS/RS
		5			11,6%		-	341			BS
	2	1			11,7%		-	371			RS
		2	20°C, 65%RH	20°C, 65%RH	11,8%	Just before the specimens were loaded to failure	-	370			RS
		3			12,4%		-	391	375	3,7	RS
		4			11,6%		-	388			RS
		5			12,4%		-	357			RS
B	1	1			7,7%		-	307			BS/RS
		2			7,9%		-	292			BS/RS
		3			8,1%		-	260	290	6,8	BS/RS
		4			7,6%		-	285			BS
		5			7,9%		-	308			BS/RS
	2	1			8,0%		-	300			RS
		2		20°C, 30%RH	7,8%		-	322			RS
		3			7,9%		-	329	315	4,5	RS
		4			7,8%		-	300			RS
		5			7,9%		-	325			RS
C	1	1			7,8%		Small crack at one row	259			BS
		2			9,1%		Fabrication error	-			-
		3			8,1%	Just before the climate was changed	-	239	248	3,3	BS/RS
		4			8,1%		-	248			BS
		5			7,6%		-	247			BS/RS
	2	1			8,3%		Crack through two rows	277			RS
		2			8,1%		Small crack at end grain	264			RS
		3			8,2%		-	264	277	5,5	RS
		4			8,3%		Crack through one row	280			RS
		5			7,8%		Crack through one row	301			RS

*Step1: storage in standard climate until moisture equilibrium was reached (~12% MC)

**Step2: storage in climate chambers (110 days) before the specimens were loaded to failure

Note: COV = Coeffeicient of variation; BS = Block-shear failure; RS = Row-shear-out failure

Type 3

Category	Specimen	Days of drying in climate chambers (1day=24hours)	Density at 12 % MC (kg/m^3)	Load-bearing capacity (kN)	Mean capacity (kN)	COV (%)	Characteristic values Experimental (kN)	Characteristic values EC5 (kN)	Max plastic disp.* (mm)	Mean plastic disp. (mm)
A1	1	0	407	56	59	2,6	50	33	10,25	6,38
	2	0	480	59					3,47	
	3	0	464	60					3,67	
	4	0	454	60					3,87	
	5	0	420	60					10,65	
B1	1	3	461	54	56	5,4	47	33	1,1	2,07
	2	3	403	59					3,89	
	3	3	447	53					0,98	
	4	3	444	57					2,3	
B2	1	7	421	49	51	10,7	42	33	1,35	1,38
	2	7	435	45					1,57	
	3	7	480	51					0,7	
	4	7	475	58					1,89	
B3	1	14	485	51	54	9,5	46	33	0,36	1,25
	2	14	435	57					2,15	
	3	14	448	49					0,59	
	4	14	450	60					1,9	
B4	1	30	450	54	50	5,0	42	33	0,59	0,83
	2	30	426	48					0,97	
	3	30	402	49					1,02	
	4	30	480	49					0,72	
B5	1	60	401	52	52	5,5	44	33	0,68	0,74
	2	60	420	51					0,47	
	3	60	480	56					1,35	
	4	60	460	49					0,46	

Note: COV = Coefficient of variation; EC5 = Calculated according to Eurocode 5 (2004)

*Plastic displacements = Tot. displacements - Elastic displacements

Type 1 and 2

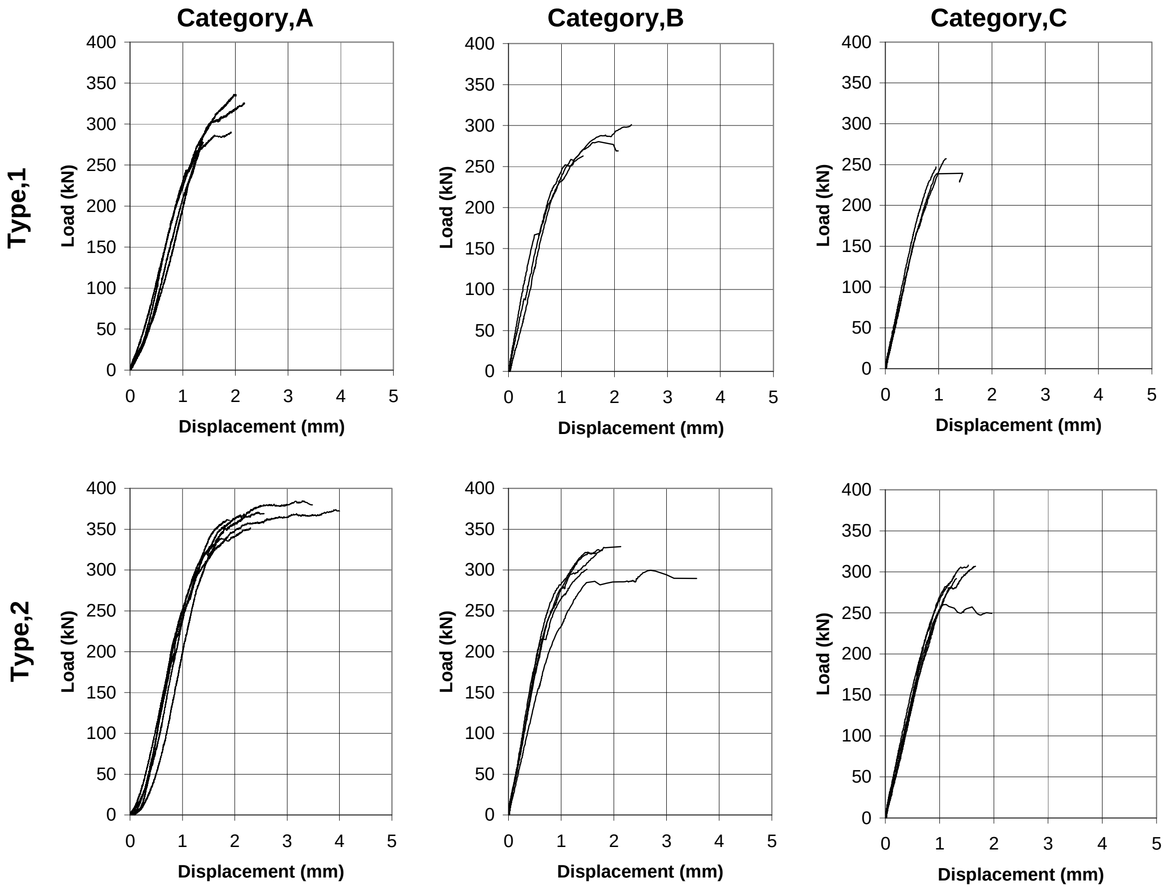
Category,A
Category,B
Category,C
Type,1
Type,2
Load (kN)
Displacement (mm)
0
50
100
150
200
250
300
350
400
0
1
2
3
4
5

Type 3

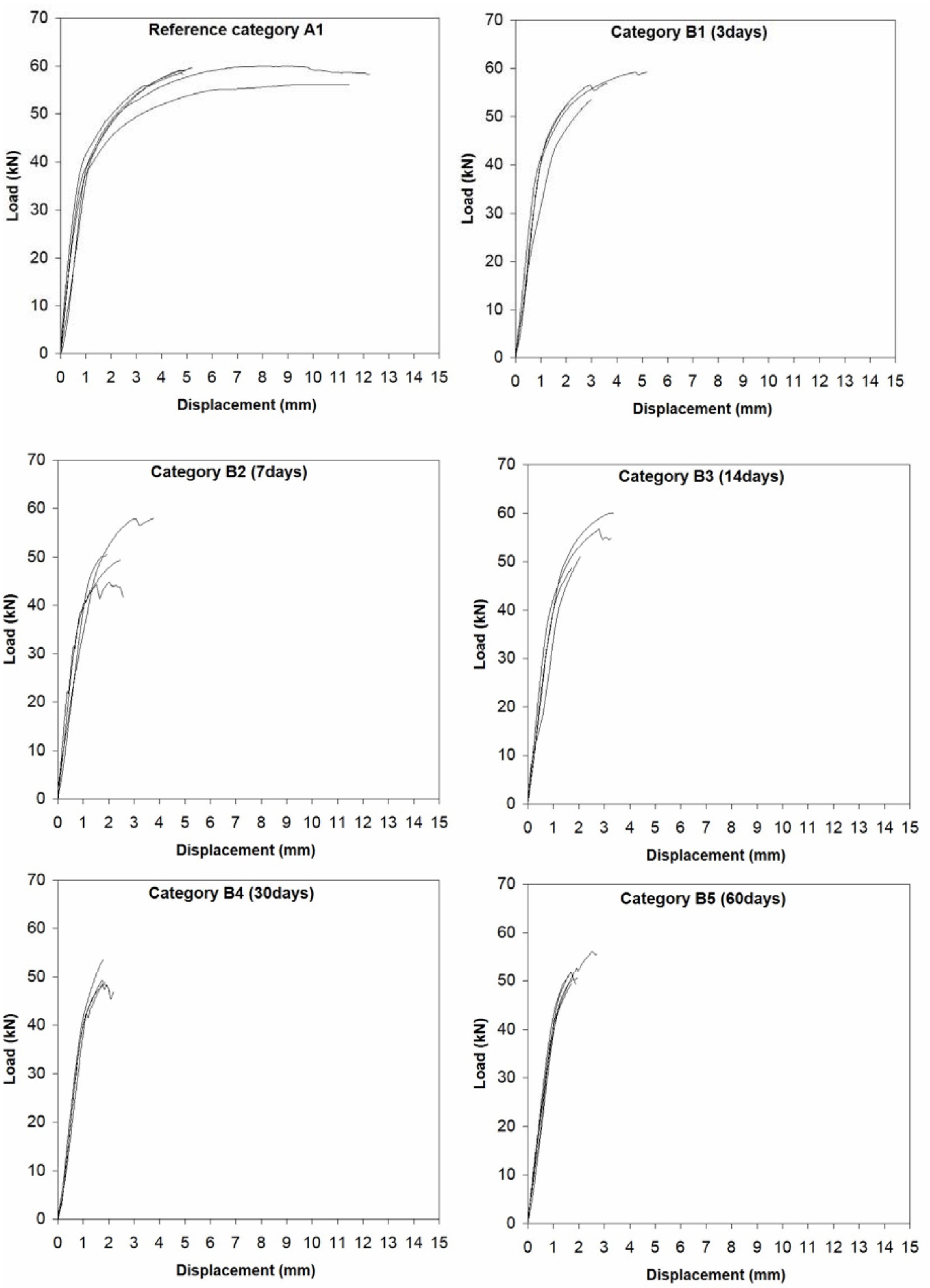
Reference category A1
Category B1 (3days)
Category B2 (7days)
Category B3 (14days)
Category B4 (30days)
Category B5 (60days)
Load (kN)
Displacement (mm)
0 10 20 30 40 50 60 70
0 1 2 3 4 5 6 7 8 9 10 11 12 13 14 15